The Influence of Microstructure on Hydrogen Diffusion and Embrittlement of Multiphase Fine-Grained Steels with Increased Plasticity and Strength

A. Begić Hadžipašić, * **J. Malina, and M. Malina**
University of Zagreb, Faculty of Metallurgy,
Aleja narodnih heroja 3, 44103 Sisak, Croatia

The influence of microstructure on hydrogen diffusion and embrittlement of multiphase fine-grained structural steels with increased plasticity and strength was studied with electrochemical experiments which provide the hydrogenation of specimens in conditions simulating practice requirements.

By means of all experimental data obtained from permeation experiments, mechanical investigations, SEM and EDS analyses, TRIP steel has shown greater resistance to hydrogen embrittlement than DP steel, testified by lower index of hydrogen embrittlement, lower diffusion coefficient, less inclusions and favourable microstructure with residual austenite. Namely, the residual austenite in the aspect of hydrogen embrittlement is a favourable phase in relation to martensite, because of its higher solubility of carbon and hydrogen and lower hardness. Therefore, TRIP steel could be considered the more suitable structural material than DP steel for application in conditions where contact with hydrogen is inevitable.

Key words:
Fine-grained HSLA steels, hydrogen diffusion, electrochemical methods, microstructure, mechanical properties, hydrogen embrittlement

Introduction

Automobiles play an important role in our daily life. This demands the incessant attempts to reduce their production cost in line with the innovation of production technology. At the same time, measures are being taken toward the reduction of fuel cost and the improvement of safety so that eagerly-pursued harmony with the social and natural environment can be established. It is safe to say that thin steel sheets for automobiles have made progress in responding to the market needs. In recent years, it has become one of the most important tasks for automobiles to make the reduction in weight of auto bodies compatible with the improvement of crashworthiness, particularly with the aim of reducing CO_2 gas emissions by improving fuel consumption.[1,2]

Conventional high strength steels were manufactured by adding alloying elements such as Nb, Ti, V, and/or P in low carbon or IF (interstitial free) steels. These steels can be manufactured under relatively simple processing conditions and have been applied widely for weight reduction. However, as the demands for weight reduction are further increased, new families of high strength steels have been developed. These new steel grades include DP (dual phase), TRIP (transformation induced plasticity), FB (ferrite-bainite), CP (complex phase) and TWIP (twin induced plasticity) steels.[3–6] The critical part of steel manufacturing is to control the processing conditions so that the microstructure and, hence, the strength-elongation balance could be optimized. This demand can be achieved in a plate by using the thermomechanically controlled process (TMCP).[5,7]

The reliability of structures or other components of mechanical equipment depends not only on the applied load but also on the conditions at which they operate. This could be a corrosive or severe environment at which the material could lose mechanical properties, thereby causing premature failures.[8–10] There are different forms of degradation, one of which is the weakening of the material due to hydrogen, otherwise known as hydrogen embrittlement (HE). Hydrogen embrittlement is the form of environmentally assisted failure caused by the action of hydrogen often in combination with residual or applied stress resulting in the reduction of load bearing capacity of a component and premature failure.[11,12]

The impact or degradation due to hydrogen may vary with composition, microstructure, and stress levels of the material in service. Metallurgical defects and imperfections such as voids, dislocations, vacancies etc., can act as trapping sites, and thereby play a crucial role in the uptake and transport of hydrogen in a material.[13–15] The concentra-

tion of hydrogen traps in the material determines the level or degree to which the material can suffer. The concentration is a function of the diffusion coefficient, which can be determined experimentally by different methods. The method that has greater acceptance in determining the diffusion in steel materials is the hydrogen permeation technique developed by Devanathan and Stachurski.[16–18] This method is based on the use of a twin or double electrolytic cell. Hydrogen is introduced in one side of a metal membrane by cathodic reduction while the other side of the membrane of the second is filled with an alkaline electrolyte such as sodium hydroxide with enough potential to oxidize any hydrogen coming through the membrane. This experimental set-up formally called Devanathan-Stachurski (DS) double cell is employed extensively to determine the hydrogen permeation rate through metallic membranes.

The above-mentioned modern class of high strength steels could also be used for the construction of bridges, tunnels and buildings, where excellent mechanical properties can be deteriorated in interaction with an aggressive medium saturated with hydrogen. Thus, in this work the influence of microstructure on the diffusion and embrittlement of DP and TRIP steel was investigated.

Experimental

Two types of steel were used for the investigation: dual phase steel marked DP and multiphase TRIP steel marked K. The sample marked DP was representative of low-carbon high-strength hot-rolled strip of dual phase steel, produced by thermomechanically controlled process on modern CSP plant for control strip production.

The sample marked K is representative of multiphase TRIP steel showing transformation induced plasticity effect (TRIP) obtained by special thermomechanical process.

Chemical composition of examined materials is given in Table 1 in order to gain insight into their quality.

It can be seen from Table 1 that these materials have low content of sulphur and phosphor, which provides high purity and quality of examined steel materials, because it minimizes the possibility of creation of sulphides and other inclusions.

The application of investigated steels is primarily in automobile industry, because of their high strength, increased deformation ability and absorption of high impact energy ("stretch effect").

In order to investigate the tendency toward hydrogen embrittlement, it is necessary to hydrogenate the samples. The penetration of hydrogen atoms through steel materials can be accelerated by the simple laboratory procedure of electrochemical examination of hydrogen diffusion in ferrous materials.[16] For permeation experiments the samples were cut from steel sheet of original thickness into plates with following dimensions: sample DP = $(5 \times 8 \times 0.15)$ cm and sample K = $(5 \times 8 \times 0.12)$ cm. The anodic (exit) side of the samples was coated with nickel, because the experimental conditions (medium and electrode potential) were controlled so the surface at the oxidation side of metallic membrane remained passive or corrosion resistant. The coating with nickel was performed at ambient temperature through 55 minutes and with current density of 0.5 A dm^{-2}. Before each measurement, the entry side of the sample was grounded with emery paper to a 600 grit finish, rinsed in distilled water, and degreased in ethanol.

The experimental device for monitoring hydrogen diffusion through the metallic membrane consisted of a cell for hydrogen charging (entry part) and an oxidation cell (exit part), separated with a thin steel plate (sample-working electrode).[19] The entry side of the sample is hydrogenated, so it is placed in contact with the cell filled with 2 mol L^{-1} H_2SO_4 deaerated with nitrogen, while the anodic side is placed next to the anodic (exit) part filled

T a b l e   1 – *Chemical composition of examined materials (w/%)*

Type of steel	DP steel	TRIP steel
Sample	DP	K
C	0.05	0.11
Mn	1.23	1.56
Si	0.42	1.18
P	0.012	0.009
S	0.003	0.001
Al	0.033	0.054
N	0.0085	–
Cu	0.16	0.01
Nb	0.002	0.003
Ti	–	0.007
Mo	0.01	0.001
V	–	0.003
Cr	0.66	0.03
Ni	0.05	0.01
Sn	0.008	0.002
As	–	0.003

with 1 mol L^{-1} NaOH. In the anodic part were placed saturated calomel electrode (SCE) as reference electrode and Pt-electrode as counter electrode. The potential of steel membrane is maintained by Parstat Potentiostat/Galvanostat (Princeton Applied Research, USA) Model 2273 in the passivity area: + 200 mV vs. SCE.

In the entry part of the experimental device the hydrogen evolution occurs, which in one part recombines into the hydrogen molecule and releases in the form of gaseous hydrogen, while the second part of hydrogen diffuses through the steel membrane to the anodic part and oxidizes in H$^+$-ions by the influence of applied potential. The current flow between the steel membrane (working electrode) and counter electrode (Pt-electrode) is registered at potentiostat as permeation current $I/\mu A$, which presents the measure for the amount of hydrogen that diffuses through the steel membrane.

Because the samples for permeation experiments were not of same thickness, the given values reduce to normalized values and display graphically in the form of normalized flux of atomic hydrogen $J(t)/J_{ss}$ against the normalized time τ. On the basis of such presentation a mathematical modeling of hydrogen diffusion could be performed. The mathematical models for study of permeation transient through metallic membrane were developed for potentiostatic and galvanostatic charging on the basis of Fick's laws.[20] Two models were used for mathematical modeling of hydrogen diffusion in order to find out which model fits experimental diffusion curves of examined materials:

– CC model of constant concentration:

$$\frac{I_t}{I_\infty} = \frac{2}{(\pi\tau)^{1/2}} \sum_{n=0}^{\infty} \exp\left[-\frac{(2n+1)^2}{4\tau}\right] \qquad (1)$$

– CF model of constant flux:

$$\frac{I_t}{I_\infty} = 1 - \frac{4}{\pi} \sum_{n=0}^{\infty} \frac{(-1)^n}{(2n+1)} \exp\left[-\frac{(2n+1)^2 \pi^2 \tau}{4}\right] \qquad (2)$$

A degradation of material caused by hydrogen absorption through corrosion reaction could be evaluated on the basis of changes in mechanical properties of hydrogenated specimens. For this purpose, specimens for tensile testing were cut in rolling direction[21] and grounded with emery paper to a 600 grit finish. The sample was then rinsed in distilled water, degreased in ethanol and immersed into 2 mol L^{-1} H$_2$SO$_4$. In charging cell, saturated calomel electrode as reference electrode and Pt-net as counter electrode were placed next to the working electrode.[22]

In order to accelerate the charging of specimens, cathodic polarization by "Parstat" Potentiostat/Galvanostat Model 2273 was carried out for four hours at potential of –700 mV vs. SCE and at temperature $T = (19 \pm 2)$ °C. After cathodic polarization, the specimens were investigated by "Instron" tensile testing machine type 1196.

The period between polarization and mechanical testing was no longer than 30 minutes, so it could be assumed that absorbed hydrogen had significant influence at given values during investigation.

For the purpose of metallographic investigations of microstructural characteristics of non-hydrogenated steels, the samples were cut in rolling direction and pressed by "SimpliMet®" machine for hot pressing of samples. The samples were then grounded (emery paper No. 400, 500, 600 and 800 grit) and polished by the "Buehler" automatic device for grounding and polishing. Such prepared samples were etched by nital (5 % HNO$_3$ in ethanol) and their microstructure was recorded by optical microscope with "Olympus GX 51" digital camera with system for automated picture analysis (AnalySIS® Materials Research Lab).

SEM analysis of examined samples was carried out by scanning electron microscope "Tescan Vega LSH" (Czech Republic) equipped with "Bruker" EDS spectrometer. SEM micrographs of examined samples were obtained by technique of secondary scattered electrons (SEI). By the method of energy disperse spectrometry (EDS), the electron beam was governed on the globular and elongated inclusions, where characteristic spectrums and chemical compositions of inclusions were obtained.

Results and discussion

On the basis of electrochemical diffusion measurements and taking into consideration the registered hydrogen current at the exit side of membrane $I/\mu A$ and working area A/cm^2, the permeation current density of atomic hydrogen $i(t)$ was calculated according to the following equation;[18]

$$i = \frac{I}{A} \ [\mu A \ cm^{-2}] \qquad (3)$$

and displayed as the function of diffusion time $i = f(t)$ for both tested samples (Fig. 1).

By the analysis of obtained results from diagrams $i = f(t)$, diffusion coefficient could be calculated for each steel by the Fick's laws. For this purpose, atomic hydrogen permeation current density in steady-state i_{ss}, defined as asymptotic value at permeation curve, is determined. The i_{ss} value is es-
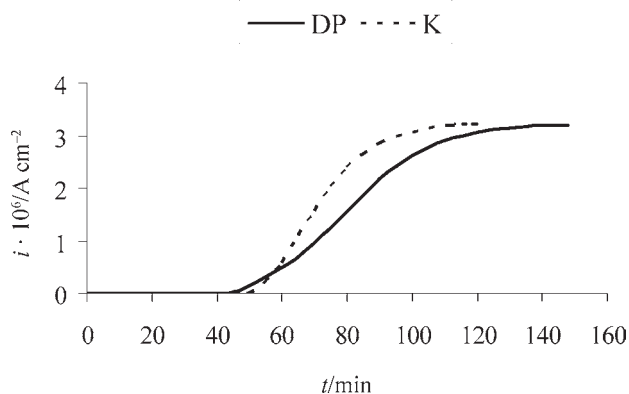
F i g . 1 – *Permeation current density of atomic hydrogen against diffusion time through steel membrane of dual phase steel marked DP and TRIP steel marked K*

tablished at the moment when all H-atoms that penetrate into the membrane ease out at the opposite side, where steady-state atomic hydrogen permeation flux is accomplished. In addition, time delay t_{lag} is determined, defined as time necessary to obtain 63 % of steady-state atomic hydrogen permeation current density.

Fig. 1 shows that hydrogen absorbed at the entry side of the dual phase steel needs 42 minutes to breakdown at the other side of the membrane. When all traps are filled, steady-state flux of atomic hydrogen is established at the exit side of membrane, which can be seen as i_{ss} at the permeation curve after 148 minutes. TRIP steel needs 50 minutes to breakdown at the other side of membrane, while steady-state flux of atomic hydrogen is established already after 120 minutes. If irreversible traps exist in sample, hydrogen atoms are tightly bonded and they can drive out from the sample only at temperature 305–750 °C. However, in reversible traps hydrogen atoms are weakly bonded and can move by diffusion for a long time through a crystal lattice until they breakdown at the other side of membrane.[23] Such hydrogen is called diffusible hydrogen and it consists of hydrogen trapped in reversible traps and hydrogen remained after production. The hydrogen trapped in reversible traps can drive out from the sample already at room temperature, and completely at temperature 112–270 °C. Diffusible hydrogen is dangerous because it can move through a crystal lattice for a long time until it finds a suitable place, but it can also move from one place to another and cause additional stress in a crystal lattice and finally a delayed fracture.

On the basis of obtained results, the following diffusion parameters have been calculated:[18] diffusion coefficient D_{eff}, amount of hydrogen atoms in a steady-state that passed through a metal membrane $n(H_2)$, volume of hydrogen atoms at steady-state

that passed through a metal membrane $V(H_2)$, atomic hydrogen permeation flux at steady-state J_{ss} and summation of the sub-surface concentration of hydrogen in interstitial lattice sites and reversible trap sites on the charging side of the sample C_{0R}. Calculated parameters can be connected to a number of reversible traps in examined material N_T, which is calculated as:[24]

$$N_T = N_L \left(\frac{D_L}{D_{eff}} - 1 \right) e^{-\frac{E_b}{RT}} \ [\text{cm}^{-3}] \qquad (4)$$

where N_L is the number of reversible traps in α-Fe ($7.52 \cdot 10^{22}$ cm^{-3}), D_L is the lattice diffusion coefficient of atomic hydrogen without traps ($1.28 \cdot 10^{-4}$ cm^2 s^{-1}), D_{eff} is the effective diffusion coefficient, E_b is the bond energy (0.3 eV), R is the universal gas constant and T is the temperature.

Above-mentioned diffusion parameters were calculated as arithmetic mean of three measurements for both examined samples and displayed in Table 2.

T a b l e 2 – *Hydrogen diffusion parameters of examined steel materials*

Type of steel	DP steel	TRIP steel
Sample	DP	K
E_{corr}/mV vs SCE	–262	–312
L/cm	0.15	0.12
i_{ss}/μA cm^{-2}	3.27	3.24
t_{lag}/s	5031	4421
$n(H_2) \cdot 10^6$/mol cm^{-2}	0.14	0.11
$V(H_2) \cdot 10^3$/cm^3 H$_2$ cm^{-2}	3.18	2.56
$D_{eff} \cdot 10^7$/cm^2 s^{-1}	7.46	5.71
$J_{ss} \cdot 10^{11}$/mol cm^{-2} s^{-1}	3.39	3.36
$C_{0R} \cdot 10^6$/mol H cm^{-3}	6.82	7.22
$N_T \cdot 10^{-25}$/cm^{-3}	1.28	1.68

From the values in Table 2 it can be noticed that diffusion parameters are lower by three orders of magnitude than that in crystal lattice of α-Fe ($D_{Fe} = 1.28 \cdot 10^{-4}$ cm^2 s^{-1}),[17] which means that lots of traps are present that slow down the transport of H-atoms through a membrane. The number of reversible traps in the examined materials was in the order of magnitude of 10^{25}, which confirms the above-mentioned fact. However, it can be noticed that N_T is lower in dual phase steel than in TRIP steel, resulting in lower C_{0R} and increased D_{eff}. Namely, it is known that decreasing of D_{eff} and in-

creasing of C_{0R} strongly depends on hydrogen trapping, and traps are most frequently various defects in the material such as dislocations, grain boundaries, etc.[13–15,25,26]

For the purpose of ranking the samples according to permeation characteristics and mathematical modeling of hydrogen diffusion, the given results were reduced to normalized values and shown as normalized flux of atomic hydrogen $J(t)/J_{ss}$ against the normalized time τ.[18] Mathematical modeling of hydrogen diffusion of examined dual phase steel and TRIP steel is presented in Fig. 2.
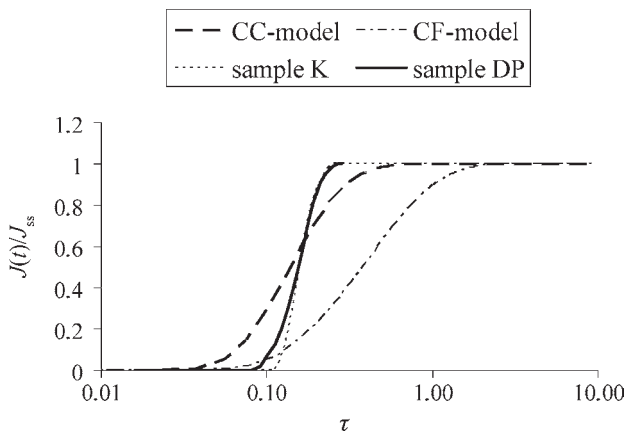

F i g . 2 – *Mathematical modeling of normalized flux of atomic hydrogen against the normalized time for dual phase steel marked DP and TRIP steel marked K*

Fig. 2 shows that the curve of the normalized flux of atomic hydrogen against the normalized time for dual phase steel has a smooth slope, which means that hydrogen atoms need more time to travel to the other side of membrane. In other words, hydrogen absorption in traps of that material is slower than in TRIP steel, because irreversible traps exist besides reversible traps and they permanently bond absorbed hydrogen. In contrast, the steeper curve for TRIP steel indicates less irreversible traps (MnS-inclusions, carbides) than in dual phase steel.[18]

Furthermore, Fig. 2 indicates that the normalized curves of both samples are fitted more to the CC-model, meaning that experimental curves of dual phase steel and TRIP steel follow the initial and boundary conditions determined according to model of constant concentration.

The mechanical properties of hydrogenated and nonhydrogenated specimens are presented in Table 3. Table 3 also gives the hydrogen embrittlement index HE, which is the indicator of hydrogen embrittlement calculated according to following equation:

$$HE = \frac{Z(air) - Z(H_{abs})}{Z(air)} \cdot 100 \ [\%] \qquad (5)$$

where $Z(air)$ is the contraction of nonhydrogenated specimen and $Z(H_{abs})$ is the contraction of hydrogenated specimen.

It can be seen from Table 3 that both samples show certain deterioration of mechanical properties after hydrogenation, indicating the fact that absorbed hydrogen had a negative influence on mechanical properties of examined materials. It is very important to notice that the negative effect of absorbed hydrogen especially manifests on elongation and contraction. Namely, the hydrogen does not influence much yield strength and tensile strength, but significantly lowers the elongation and contraction. However, it is important to notice that before hydrogenation the elongation of TRIP steel was approximately two times higher than that of dual phase steel. Furthermore, TRIP steel has shown higher elongation after hydrogenation than dual phase steel before hydrogenation, indicating that although hydrogen in TRIP steel lowers the elongation, that value is acceptable. Also, TRIP steel has

T a b l e 3 – *Mechanical properties of examined materials before and after hydrogenation*

Type of steel	Sample	Yield strength R_e/MPa	Tensile strength R_m/MPa	Elongation A/%	Contraction Z/%	Index of hydrogen embrittlement HE/%
DP steel	DP	Before hydrogenation				58.58
		545	628	24.0	63.5	
		After hydrogenation				
		468	628	20.0	26.3	
TRIP steel	K	Before hydrogenation				17.92
		398	644	45.7	62.5	
		After hydrogenation				
		387	593	30.3	51.3	

shown lower hydrogen embrittlement index, which is evidence that TRIP steel is more resistant to hydrogen embrittlement than the examined dual phase steel. In other words, the examined TRIP steel has a larger and uniform elongation, which makes it more resistant material, because it can absorb much more energy under loading. However, TRIP steel is used for construction of parts strongly capable of absorbing impact energy.[27]

Such behavior of examined materials is closely related to their chemical composition and microstructure. Optical micrographs of microstructure of examined samples etched by nital are presented in Fig. 3.
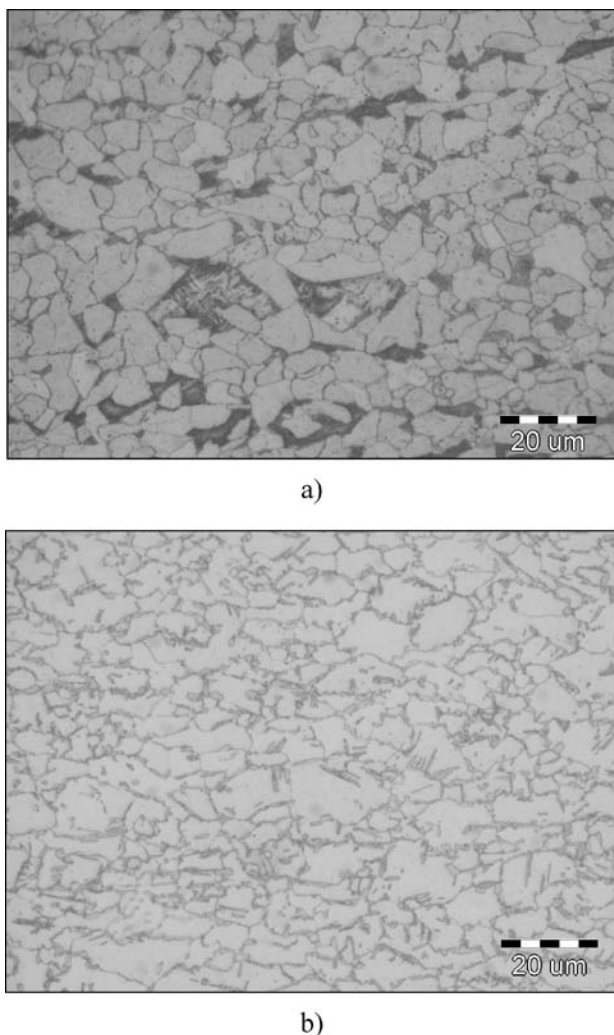

a)

b)

F i g . 3 – *Optical micrograph of microstructure of: a) dual phase steel marked DP and b) TRIP steel marked K*

Fig. 3 shows that both steels have extremely fine-grained microstructure, which cannot be analyzed according to micrographs registered by optical microscope with the highest magnification 1000x. Therefore, the microstructure of examined materials has been analyzed by scanning electron
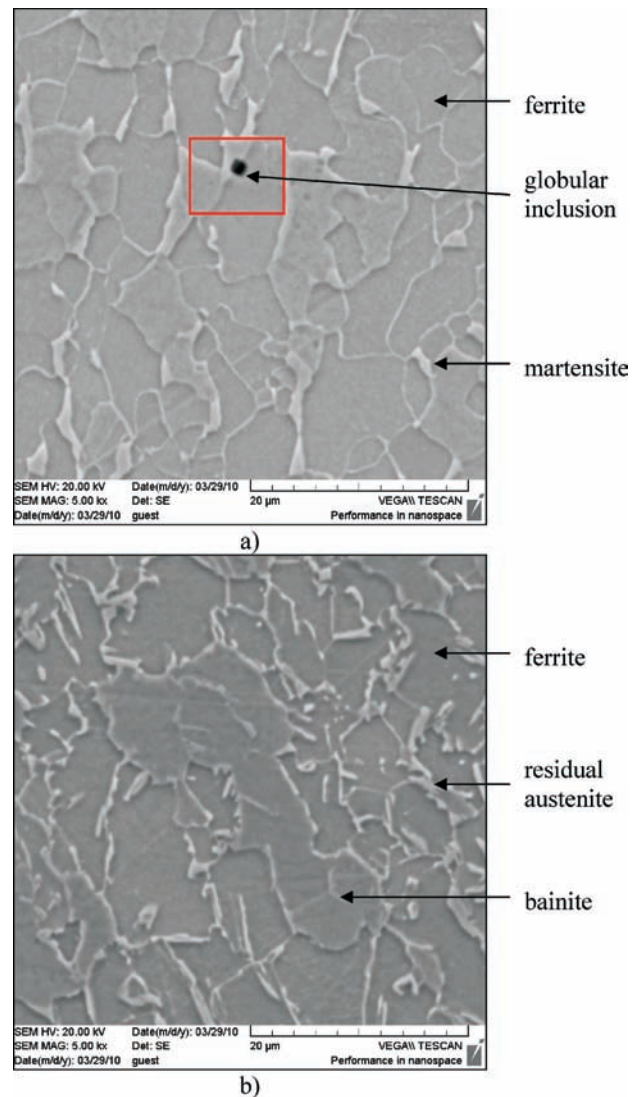

a)

b)

F i g . 4 – *SEM micrograph of microstructure of: a) dual phase steel marked DP and b) TRIP steel marked K*

microscope, where magnification is much larger (Fig. 4).

It can be noticed from Fig. 4 that sample DP presents dual phase steel consisting of ferrite and islands of martensite. Since the microstructure is fine-grained (grain size No. 12),[28] high density of dislocations and numerous grain boundaries provide longer travel of atomic hydrogen through a crystal lattice of examined material and therefore slower breakdown of hydrogen at opposite side of membrane.

Namely, the setting of DP microstructure first requires the formation of a sufficient amount of soft ferrite. Fig. 5 shows that for this purpose the austenite is finish rolled shortly above or in the range of the beginning polymorphic $\gamma \rightarrow \alpha$ transformation.[5] If necessary, rolling may be followed by intensive cooling to transformation temperature. The trans-
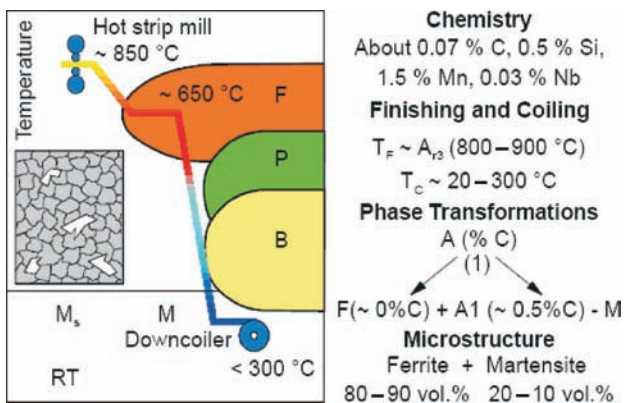
F i g . 5 − *Schematic review of phase transformations in production of dual phase steel*[5]

F i g . 6 − *Schematic review of phase transformations in production of TRIP steel*[5]

formation kinetics depends on the undercooling and on the microstructure of the hot-deformed austenite (residual deformation, austenitic grain size, etc.).

During transformation from austenite into ferrite, carbon is separated between the two solid solutions. Since ferrite dissolves much less carbon, this element is concentrated in the remaining austenite. The austenitic areas are enriched with carbon and may undergo martensitic transformation already at cooling rates of 20 to 30 °C s^{-1}; the hot strip is coiled below the martensite starting temperature (≤ 300 °C).

It is very important here to note that the strengthening mechanism of dual phase steel is accomplished by increasing the content of manganese and chromium. Namely, the analyzed dual phase steel is microalloyed with chromium (0.66 %). Normally, chromium is known as austenite stabilizer and it decreases the cooling rate needed for transformation without diffusion.[4,27] That helps the formation of martensite, which is an unfavorable phase in the microstructure from the hydrogen embrittlement aspect. Manganese is mostly added to prevent the perlite transformation, which then allows the formation of martensite or bainite.[4,27]

Therefore, the greater resistance of TRIP steel towards hydrogen embrittlement can be explained by its favorable microstructure-without martensite. Fig. 4b presents fine-grained microstructure (grain size No. 13)[28] consisting of three phases: ferrite, bainite and residual austenite. Namely, the production of multiphase steel showing transformation induced plasticity effect (TRIP) calls for metastable (residual) austenite in the finished product (Fig. 6).[5]

To achieve this, the martensite temperature must be lowered to below room temperature. Again, this can be done by carbon enrichment, but in this case, the carbon concentration must be significantly higher than in DP steel. Therefore, the initial carbon content is increased to approx. 0.2 %
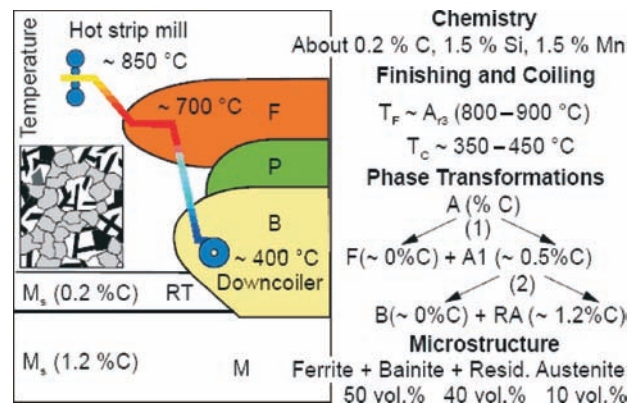
and two enrichment stages in the ferritic and bainitic ranges are introduced (see Fig. 6). In the ferritic range, the carbon concentration in the austenite goes up to approx. 0.5 % and in the bainitic range to approx. 1.2 %. The decisive step for setting the austenite existing at room temperature takes place in the bainitic range. By setting an appropriate holding temperature and time, both an adequate amount of austenite and its required thermodynamic metastability will be set. Namely, it is known that diffusion in austenite is slower and solubility higher than in ferrite.[4] From the aspect of hydrogen embrittlement, the residual austenite is a more favorable phase than martensite, because of its higher solubility of carbon and hydrogen and lower hardness.

The desired specific transformation-behavior of TRIP steels depends on defined chemical compositions. It can be noticed from Table 1 that TRIP steel is strengthened by increasing the content of carbon, manganese and silicon, which is different from the strengthening mechanism of dual phase steel. Carbon is a highly strength-increasing alloying element that in this connection takes adequate effect already at concentrations of approx. 0.2 % for TRIP steels. Silicon and possible substitutes for it play an important role in multiphase steels.[5] Two effects of silicon as alloying element are of particular interest in TRIP steels: first, silicon is a strong ferrite stabilizer and leads to heavy formation of proeutectoid ferrite. Second, silicon suppresses the formation of cementite in the bainitic range; this is especially useful for TRIP grades. Adding approx. 1.5 % silicon ensures that an adequately high carbon concentration is set in the austenite which prevents its martensitic transformation at room temperature. This way metastable residual austenite is set.

Since irreversible traps can be various carbides and inclusions (especially MnS), they are significantly present in the examined dual phase steel.

Namely, SEM analysis of dual phase steel revealed a great number of globular inclusions dimensions from 2–10 μm and some elongated inclusions dimensions from 20–100 μm (Figs. 7 and 8). To establish the connection between the chemical composition and microstructure concerning the hydrogen embrittlement of steel materials, EDS analysis of globular inclusion in sample DP revealed the presence of (Ca, Al)-oxides, due to an increasing content of oxygen, calcium and aluminum (Fig. 7).

The formation of these complex oxides is caused by calcium treatment in ladle furnace, which leads to their increased hardness and maintains their globular shape through the forming process.[5,9,15,22] In that the other hand, elongated MnS inclusions with bigger dimensions increase anisotropic properties and the number of irreversible traps. EDS analysis of elongated inclusion in sample DP has shown an increased content of oxygen, aluminum, manganese, carbon and sulphur (Fig. 8), which indicates that (Mn, Al)-oxsisulphides and (Mn, Al)-oxicarbides are present in the examined sample.

SEM analysis also revealed that elongated inclusions were mostly found in the center of sample
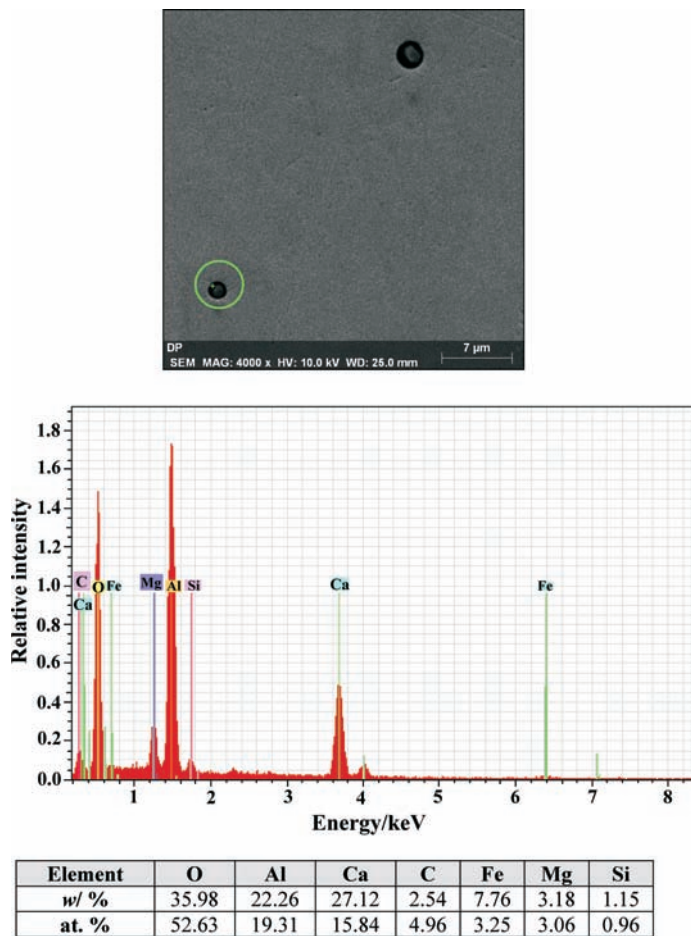

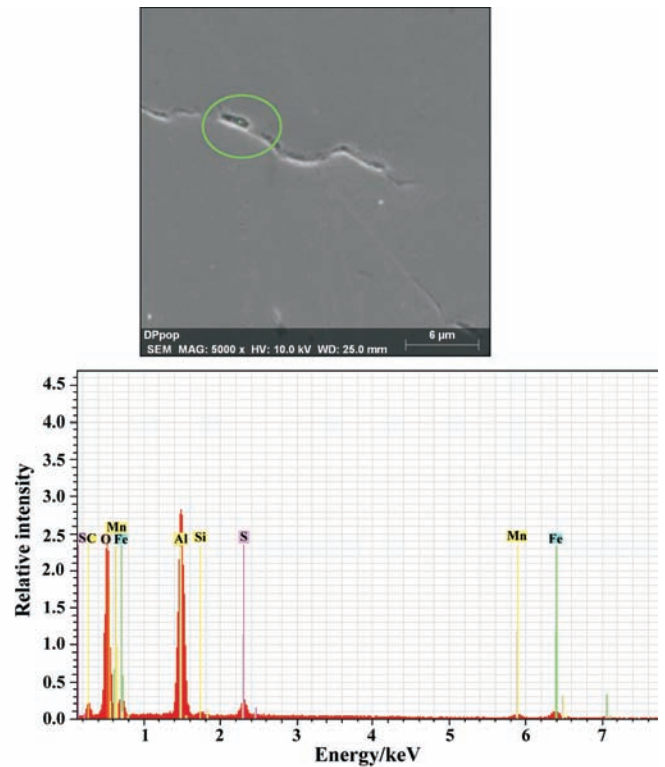| Element	O	Al	Fe	C	Mn	S	Si
w/ %	27.43	25.52	31.08	2.39	10.62	2.73	0.23
at. %	46.31	25.55	15.03	5.37	5.22	2.30	0.22

F i g . 8 − *EDS analysis of elongated inclusion in dual phase steel marked DP*

DP and in the rolling direction, because during rolling, segregation of all impurities occurs in the center of hot-rolled strip. Also, the propagation of elongated inclusions at grain boundaries was determined, because grain boundaries are favorable places for accumulation of different segregations, which form inclusions during rolling. No elongated inclusions were registered in sample of TRIP steel marked K, but there were plenty globular inclusions (Fig. 9), indicating a decreased presence of irreversible traps here. EDS analysis of globular inclusion revealed increased content of oxygen, aluminum, manganese and sulphur, which means that globular (Ca, Al, Mn)-oxisulphides are present (Fig. 9).

Observing the experimental results of examined materials, TRIP steel has shown better resistance to hydrogen embrittlement than dual phase steel, because of its different strengthening concept (on the basis of C, Mn, Si), higher elongation, smaller number of irreversible traps and lower hydrogen embrittlement index. Hence, it can be concluded that high resistance to hydrogen embrittlement of TRIP steel can be ascribed to its favorable microstructure (without martensite and without plenty inclusions) consisting of ferrite, bainite and residual austenite, which is the consequence of pro-
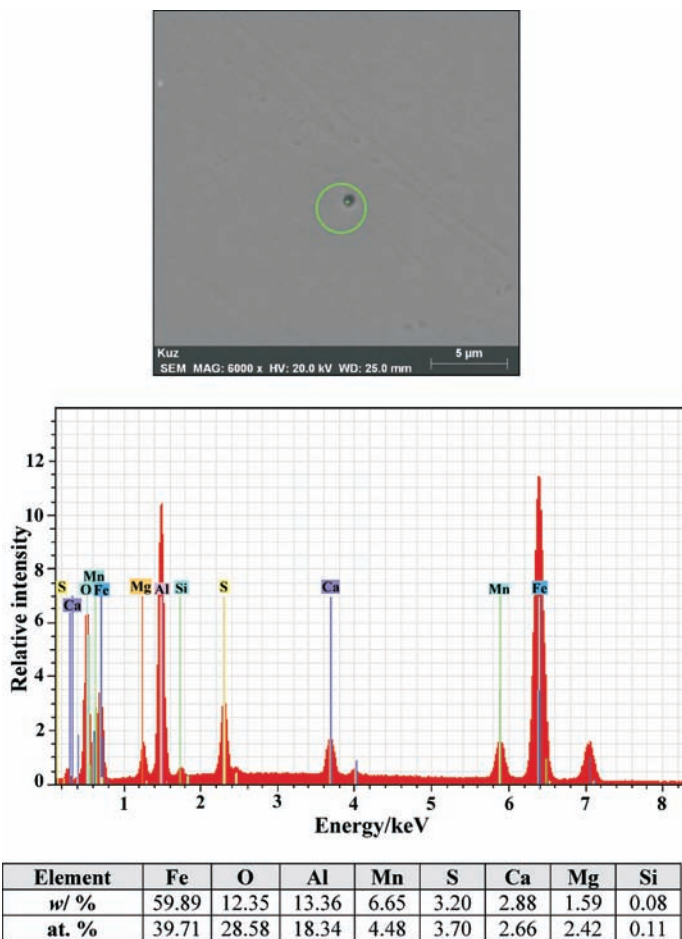

Element	O	Al	Ca	C	Fe	Mg	Si
w/ %	35.98	22.26	27.12	2.54	7.76	3.18	1.15
at. %	52.63	19.31	15.84	4.96	3.25	3.06	0.96

F i g . 7 − *EDS analysis of globular inclusion in dual phase steel marked DP*

Element	Fe	O	Al	Mn	S	Ca	Mg	Si
w/ %	59.89	12.35	13.36	6.65	3.20	2.88	1.59	0.08
at. %	39.71	28.58	18.34	4.48	3.70	2.66	2.42	0.11

F i g . 9 – *EDS analysis of globular inclusion in TRIP steel marked K*

duction with secondary metallurgy and thermo-mechanically controlled process (TMCP). Namely, from the hydrogen embrittlement aspect, residual austenite is a more favorable phase than martensite, because of its higher solubility of carbon and hydrogen and lower hardness.

Therefore, between the two examined materials of high strength and shape ability, TRIP steel can be considered a more suitable structural material of high plasticity and strength for application in conditions where contact with hydrogen is inevitable.

Conclusions

Based on the results obtained by electrochemical, mechanical, microscopic and EDS examinations, the influence of microstructure on hydrogen diffusion and embrittlement of multiphase fine-grained steel with increased plasticity and strength was studied. Two types of new generation HSLA steels, produced by modern technologies of metallurgy engineering on TMCP plants were examined: dual phase steel marked DP, and

multiphase TRIP steel marked K. The results suggest the following conclusions:

– Diffusion parameters calculated from diffusion curves through the membrane of dual phase and TRIP steel are lower by three orders of magnitude than that in crystal lattice of α-Fe, meaning that in the examined materials lots of microstructural traps were present that slowed down the transport of H-atoms.

– The permeation curve of dual phase steel has shown a smooth slope, which means that hydrogen absorption in traps of this material is slower than in TRIP steel, and that besides the reversible traps there exist irreversible traps that permanently bond absorbed hydrogen. In contrast, the steeper curve for TRIP steel indicates less irreversible traps (MnS-inclusions, carbides) than in dual phase steel.

– Since the microstructure of examined materials is fine-grained, high density of dislocations and numerous grain boundaries provide longer travel of atomic hydrogen through a crystal lattice of examined material and therefore slower breakdown of hydrogen at the opposite side of membrane.

– By mathematical modeling of given results according to Fick's diffusion law, it has shown that permeation curves of both samples are following initial and boundary conditions determined according to the CC-model of constant concentration.

– After hydrogenation the both samples have shown certain deterioration of mechanical properties, indicating the fact that absorbed hydrogen has a negative influence on mechanical properties of examined materials, especially on the elongation and contraction.

– SEM analysis of dual phase steel revealed a great number of globular and elongated inclusions (known as strong irreversible traps). EDS analysis of globular inclusion in sample DP revealed the presence of (Ca, Al)-oxides, while EDS analysis of elongated inclusion has identified the presence of (Al, Mn)-oxisulphides and (Al, Mn)-oxicarbides. SEM and EDS analysis of TRIP steel have shown only the presence of globular inclusions type of (Ca, Al, Mn)-oxisulphides.

– Dual phase steel consists of ferrite and islands of martensite. The lower resistance to hydrogen embrittlement, which results from high hydrogen embrittlement index, can be ascribed to the presence of martensite, which significantly decreases the resistance to HE.

– Microstructure of TRIP steel consists of ferrite, bainite and residual austenite. The residual austenite is a more favorable phase than martensite, because of its higher solubility of carbon and hydrogen and lower hardness.

– TRIP steel has shown better resistance to hydrogen embrittlement than dual phase steel, because of its different strengthening concept (on the basis of C, Mn, Si), smaller number of irreversible traps and higher elongation. On the other hand, it is important to note that before hydrogenation the elongation of TRIP steel was approximately two times higher than that of dual phase steel. Furthermore, TRIP steel has shown higher elongation after hydrogenation than dual phase steel before hydrogenation, meaning that although hydrogen in TRIP steel lowers the elongation, that value is acceptable.

– On the basis of all experimental results, it can be concluded that TRIP steel has better resistance to hydrogen embrittlement than dual phase steel, testified by the lower hydrogen embrittlement index. It can be ascribed to its production technology with thermomechanical treatment, where the obtained microstructure has the ability to suffer a great working load and absorb hydrogen without significant changes in elongation or shape ability. Therefore, between the two examined materials of high strength, TRIP steel can be considered a more suitable structural material for application in conditions where contact with hydrogen is inevitable.

ACKNOWLEDGMENT

List of symbols

A – elongation, %

A – area of steel membrane (sample), cm^2

C_{0R} – summation of the sub-surface concentration of hydrogen in interstitial lattice sites and reversible trap sites on the charging side of the sample, mol H cm^{-3}

D_{eff} – effective diffusion coefficient, cm^2 s^{-1}

D_L – lattice diffusion coefficient of atomic hydrogen without traps, cm^2 s^{-1}

E_b – bond energy, eV

E_{corr} – corrosion potential, mV

F – Faraday's constant, A s mol^{-1}

I – current, A

$I(t)$ – time-dependent current, A

I_{ss} – steady-state current, A

i – permeation current density of atomic hydrogen, A cm^{-2}

i_{ss} – permeation current density of atomic hydrogen at steady-state, A cm^{-2}

$J(t)$ – time-dependent atomic hydrogen permeation flux, mol cm^{-2} s^{-1}

J_{ss} – atomic hydrogen permeation flux at steady-state, mol cm^{-2} s^{-1}

$J(t)/J_{ss}$ – normalized flux of atomic hydrogen

L – membrane (sample) thickness, cm

M_s – martensite starting temperature, °C

N_L – number of reversible traps in α-Fe, cm^{-3}

N_T – number of reversible traps in examined material, cm^{-3}

$n(H_2)$ – amount of hydrogen atoms in a steady-state that passed through a metal membrane, mol cm^{-2}

R – universal gas constant, J mol^{-1} K^{-1}

R_e – yield strength, MPa

R_m – tensile strength, MPa

T – temperature, °C

t – time, min

t_{lag} – time delay, s

$V(H_2)$ – volume of hydrogen atoms in a steady-state that passed through a metal membrane, cm^3 H$_2$ cm^{-2}

w – mass fraction, %

Z – contraction, %

z – number of exchanged electrons

γ – austenitic phase in Fe-Fe$_3$C diagram

ε – strain, %

σ – stress, MPa

τ – normalized time

List of abbreviations

B – bainite

CC-model – constant concentration model

CF-model – constant flux model

CP steel – complex phase steel

CSP – compact strip production

DP steel – dual phase steel

DS-cell – Devanathan-Stachurski cell

EDS – energy dispersive spectrometer

F – ferrite

FB steel – ferrite-bainite steel

HE – hydrogen embrittlement

HSLA steel – high strength low-alloyed steel

M – martensite

P – perlite

SEM – scanning electron microscope

TMCP – thermo-mechanically controlled process

TRIP – transformation induced plasticity

TWIP steel – twinning induced plasticity steel

SCE – saturated calomel electrode

References

1. *Takahashi, M.,* Development of High Strength Steels for Automobiles, Nippon steel technical report No. 88 (2003) 2.

2. *Brass, A. M., Chene, J.,* Corrosion Science **48** (2006) 3222.

3. *Zrnik, J., Mamuzić, I., Dobatkin, S. V.,* Metalurgija **45** (4) (2006) 323.

4. *Parish, C.,* Fundamental Study of Phase Transformations in Si-Al TRIP Steels, Master Thesis, University of Pittsburg, Pittsburg, 2003.

5. *Hensger, K. E.,* Metalurgija **41** (3) (2002) 183.

6. *Hamada, A. S.,* Manufacturing, Mechanical Properties and Corrosion Behavior of High-Mn TWIP Steels, Doctoral Thesis, University of Oulu, Finland, 2007.

7. *Žáček, O., Kliber, J., Schindler, I.,* Acta Metallurgica Slovaca **12** (2006) 454.

8. *Wang, M., Akiyama, E., Tsuzaki, K.,* Corrosion Science **49** (2007) 4081.

9. *Malina, J., Malina, M., Hensger, K. E.,* Hydrogen induced embrittlement of weld on CSP steel in seawater, Proc. of the 3. International Conference Welding in Maritime Engeneering, ed. Zoran Kožuh, HDTZ, Hvar, 2004, pp. 173–181.

10. *Lunarska, E., Nikiforow, K., Sitko, E.,* Advances in Materials Science **4** (2003) 35.

11. *Dayal, R. K., Parvathavarthini, N.,* Sadhana **28** (2003) 431.

12. *Trassati, S. P., Sivieri, E., Mazza, F.,* Materials and Corrosion **56** (2005) 111.

13. *Zakroczymski, T.,* Electrochimica Acta **51** (2006) 2261.

14. *Park, Y. D., Maroef, I. S., Landau, A., Olson, D. L.,* Welding Journal (2002) 27.

15. *Malina, J., Begić Hadžipašić, A., Malina, M.,* The Influence of DP Steel Microstructure on Hydrogen Diffusivity, Proc. of the 4. International Conference Welding in Maritime Engeneering, ed. Zoran Kožuh, HDTZ, Bol, Brač, 2009, pp. 173–182.

16. *Devanathan, M. A. V., Stachurski, Z.,* Journal of Electrochemical Society **111** (1964) 619.

17. *Hadam, U., Zakroczymski, T.,* International Journal of Hydrogen Energy **34** (2009) 2449.

18. HRN EN ISO 17081:2008, Method of measurement of hydrogen permeation and determination of hydrogen uptake and transport in metals by an electrochemical technique.

19. *Begić Hadžipašić, A., Malina, J., Nižnik, Š.,* The Influence of Microstructure on Hydrogen Diffusion and Embrittlement of Dual Phase Steel, Proc. of the International Conference on Materials, Tribology, Recycling, MATRIB 2010, ed. Zdravko Schauperl, Mateja Šnajdar, HDMT, Vela Luka-Korčula, 2010, pp. 24–33.

20. *Cheng, Y. F.,* International Journal of Hydrogen Energy **32** (2007) 1269.

21. EN 10002-1:1990, Metallic Materials-Tensile Testing-Part 1: Method of Test at Ambient Temperature.

22. *Begić Hadžipašić, A., Malina, J., Malina, M.,* Strojarstvo **51** (6) (2009) 529.

23. *Engl, B., Drewes, E. J., Stich, G.,* Stahl und Eisen **117** (1997) 67.

24. *Park, G. A., Koh, S. U., Jung, H. G., Kim, K. Y.,* Corrosion Science **50** (2008) 341.

25. *Chatterjee, S.,* Transformation in TRIP-Assisted Steels: Microstructure and Properties, Doctoral Thesis, Darwin College, University of Cambridge, 2006.

26. ASTM standard E112-96e1, Standard Test Methods for Determining Average Grain Size.

27. *Nižnik, Š., Furman, Ľ.,* Metalurgija **34** (4) (1995) 129.

28. *Nižnik, Š., Zavacký, M., Janák, G., Furman, Ľ.,* Acta Metallurgica Slovaca **13** (3) (2007) 336.